

TITLE: Thermodynamics of the Tantalum-Carbon-Chlorine-Hydrogen System
Applied to the CVD of Carbide/Carbon Composite Materials*

AUTHOR(S): Robert G. Behrens, L. R. Newkirk and Terry C. Wallace

MASTER

SUBMITTED TO: To be presented at the 82nd Annual Meeting of the
American Ceramic Society, 27-30 April 1980,
Chicago, Illinois, and published in Advances in
Ceramic Science



*Work performed under the auspices of the United States Department
of Energy

By acceptance of this article, the publisher recognizes that the
U.S. Government retains a nonexclusive, royalty-free license
to publish or reproduce the published form of this contribu-
tion, or to allow others to do so, for U.S. Government pur-
poses.

The Los Alamos Scientific Laboratory agrees that the pub-
lisher identify this article as work performed under the aus-
pices of the U.S. Department of Energy.

DISTRIBUTION OF THIS REPORT

University of California



LOS ALAMOS SCIENTIFIC LABORATORY

Post Office Box 1663 Los Alamos, New Mexico 87545

An Affirmative Action/Equal Opportunity Employer

**Thermodynamics of the Tantalum-Carbon-Chlorine Hydrogen
System Applied to the CVD of Carbide/Carbon Composite Materials***

**Robert G. Behrens, L. R. Newkirk and Terry C. Wallace
University of California, Los Alamos Scientific Laboratory
Los Alamos, New Mexico 87545**

Abstract

Complex equilibrium thermodynamic calculations using the computer code SOLGASMIX-PV were performed for the Ta-Cl-H and Ta-C-Cl-H systems in order to evaluate the chemistry associated with the chemical vapor deposition of Ta, Ta₂C, and TaC on graphite yarn and woven structures. Results of the thermodynamic calculations were compared with coated materials prepared by hydrogen reduction of TaCl₅(g) and C₃H₆(g) between 1025K and 1223K using a variety of reaction gas compositions.

I. Introduction

Chemical vapor deposition (CVD) is a process in which gaseous reactants are transported to and react chemically at a heated surface to form a solid phase comprised of at least one of the elemental components of the gaseous reactants. Over the past fifteen years a considerable amount of work has been reported in the literature describing CVD techniques used to prepare a wide variety of materials

which cannot be prepared readily by other techniques due to the high temperatures required in the preparation.¹⁻⁹ In particular, CVD has been used successfully in preparing superconducting^{10,11} and semiconducting¹² compounds, solar collector and thin film alloys,^{13,14} and protective coatings of refractory metal carbides, oxides, borides, and nitrides.¹⁵⁻¹⁸

The High-Temperature Group of the Chemistry and Materials Science Division of the Los Alamos Scientific Laboratory (LASL) has been actively involved in CVD research and development over the past twenty five years. Past and present work has dealt primarily with the CVD application of protective coatings on graphite substrates for use in high-temperature environments. Specifically, past work has included the process development for CVD coating of the coolant channels (2.5 mm diam. x 1320 mm long) of Rover fuel elements with NbC or ZrC¹⁹⁻²¹ and the CVD coating of rocket-nozzle parts with co-deposited SiC and pyrographite.²²⁻²⁵ Current CVD research and development involves the preparation of uniformly vapor deposited materials on the filamentary surfaces of yarn, cloth, and woven structures for the fabrication of hot-pressed, fiber reinforced metal or refractory compound composites.²⁶⁻²⁹ Potential applications for these materials include use in high-temperature (>3200K), erosive environments;^{29,30} light-weight armor, and light-weight structural components for the use in high-temperature (1700K), oxidizing environments.

While a considerable amount of design work has been performed at LASL to establish techniques and process parameters for uniformly coating graphite filamentary assemblages with transition metal carbides, borides, and with silicon carbide and boron carbide, no prior attempt was made to evaluate the chemistry of the CVD processes using complex equilibrium thermodynamic calculations. Current work involving the CVD of tantalum and tantalum carbide on graphite yarn and cloth along with the absence of a detailed thermodynamic analysis of the Ta-Cl-H and Ta-C-Cl-H systems prompted us to calculate the CVD phase diagrams for these systems. The present paper reports the results of these calculations using the complex equilibrium code SOLGASMIX-IV.³¹ Results of

the thermodynamic calculations are compared with experiments in which Ta, TaC, and Ta₂C were deposited on graphite yarn and woven cloth as well as on other substrates as reported in the literature.

II. Thermochemical Properties and Phase Diagrams

A. The Ta-C System.

The phase diagram and thermochemical properties of the Ta-C system have been reviewed by Storms,³² Toth,³³ and Schick.³⁴ There are two intermediate phases in this system - TaC and Ta₂C - both of which exhibit homogeneity ranges. Ta₂C is believed essentially to be a line compound below 1775K while TaC exists between approximately TaC_{0.77} and TaC_{1.0} at 1775K. High-temperature thermodynamic functions for both TaC and Ta₂C have been tabulated by Schick³⁴ and more recently reviewed by Storms³² and Toth.³³ Schick gives values of $\Delta H_f^0(298.15K)$ for TaC and Ta₂C of -34.6 kcal mol⁻¹ and -47.2 kcal mol⁻¹ respectively while Toth selects values of -34.1 kcal mol⁻¹ and -49.8 kcal mol⁻¹ respectively.

B. The Ta-Cl System.

There are four known solid phases in this system: TaCl₅, TaCl₄, TaCl₃, and TaCl_{2.5}.³⁶ TaCl₃(s) is reported to have a range of homogeneity between TaCl_{2.9} and TaCl_{3.1}.³⁶ TaCl_{2.5} is believed to be the lowest solid chloride which is thermodynamically stable in the Ta-Cl system.

Thermodynamic functions for TaCl₅(s, l) have been presented in the JANAF Thermochemical Tables.³⁷ Thermodynamic functions for TaCl₄(s) and TaCl₃(s) have been calculated³⁸ from estimated heat capacity equations and an estimated value of S⁰(298.15K) reported by Schaefer and Kahlenberg.³⁹ Thermodynamic functions

for $\text{TaCl}_{2.5}(\text{s})$ were also calculated³⁸ from estimated heat capacity equations given by Barin and Knacke.⁴⁰

Thermodynamic properties for the gaseous molecules $\text{TaCl}_5(\text{g})$, $\text{TaCl}_4(\text{g})$, $\text{TaCl}_3(\text{g})$, $\text{TaCl}_2(\text{g})$, and $\text{TaCl}(\text{g})$ have been recently reviewed and evaluated.⁴¹

C. The C-H and C-H-Cl Systems.

A review of the literature was made to determine the more thermodynamically stable hydrocarbon and organic chloride gaseous molecules. We selected $\text{CH}_4(\text{g})$, $\text{C}_2\text{H}_2(\text{g})$, $\text{C}_2\text{H}_6(\text{g})$, $\text{C}_2\text{H}_4(\text{g})$, $\text{C}_3\text{H}_6(\text{g})$, $\text{C}_6\text{H}_6(\text{g})$, $\text{CCl}_4(\text{g})$, $\text{CH}_3\text{Cl}(\text{g})$, $\text{CH}_2\text{Cl}_2(\text{g})$, and $\text{CHCl}_3(\text{g})$ for use in the thermodynamic calculations. Thermodynamic functions for these molecules have been reviewed in the JANAF Thermochemical Tables¹² and in the compilation of thermodynamic data by Stull, Westrum, and Sinke.¹³

D. The Elements in Their Standard States

The standard state for tantalum and carbon was chosen to be the solid

and the standard state for H_2 and Cl_2 was taken as the ideal gas at 1 atm. pressure at all temperatures between 298.15K and 1300K. Thermodynamic functions for the elements in their standard states have been reviewed and evaluated by the JANAF tables¹² and by Hultgren et al.⁴⁴

III. Computational Procedure

The complex equilibrium code used in this work was SOLGASMIX-PV.³¹ The code was used as presented in Ref. 31 but with a modification which permitted thermodynamic data to be inputted in units of either Joules or calories. The code as presented in Ref. 31 was a modification of the code SOLGASMIX developed previously by Eriksson.⁴⁵⁻⁴⁷

In the thermodynamic calculations for the Ta-C-Cl-H system, 19 vapor species (including Ar) and 8 condensed phases were considered. Thermodynamic data used as input were the enthalpy of formation, $\Delta H_f^0(298.15K)$, and the change in the Gibbs free energy function for formation of the gaseous molecules or solid phases from the constituent elements, $-\Delta [G^0(T) - H^0(298.15K)]/T$, at the temperature of interest. Accordingly, the total Gibbs free energy of the system was calculated as the Gibbs free energy of formation using the equation

$$\Delta G_f^0/T = \Delta [G^0(T) - H^0(298.15K)]/T + \Delta H_f^0(298.15K)/T \quad (1)$$

Thermodynamic data used to prepare the input data are given in Table 1 and discussed in Sec. II above. Values of $-\Delta [G^0(T) - H^0(298.15K)]/T$ for temperatures at other than 100K intervals were obtained by interpolation.

The CVD phase diagram for the Ta-Cl-H system was computed by varying the H/Cl ratio of the input gas at a constant temperature, changing the temperature and then repeating the calculation. Similarly, the Ta-C-Cl-H CVD phase diagram was computed at a particular temperature for a constant value of H/Cl by varying the Ta/C ratio in the input gas, changing the temperature and/or the H/Cl ratio and repeating the calculations.

Details concerning the thermodynamics of CVD phase diagrams and examples of phase diagrams computed using the SOLCASMIX complex equilibrium code have been previously reported by Spear and co-workers.⁴⁹⁻⁵⁰

IV. Experimental Procedure

Coatings prepared in this work were deposited on Hitex-C graphite cloth (Woven Structures, Inc., Los Angeles, CA) woven from P223 staple yarn. The cloth had an areal density of 0.024 g cm^{-2} . Five to ten cloths, each approximately 6 cm in diameter, were supported in the deposition chamber of the CVD apparatus by a graphite baffle. Two graphite baffles, used to heat the coating gases to the desired deposition temperature, were situated above the cloths and were separated from the cloths by graphite spacers.

Deposition was carried out in an all-metal apparatus at reduced pressure (15 to 25 torr) so as to enhance vapor phase diffusion of the coating gases into the interior of the graphite yarn strands and to promote uniform deposition on all the graphite filaments of the cloth. The reduced pressure was achieved by a Nash high speed centrifugal pump using water as the pumping fluid.

For experiments involving only the deposition of tantalum metal, $\text{TaCl}_5(\text{g})$ was used as the coating gas. The $\text{TaCl}_5(\text{g})$ was formed by direct chlorination of tantalum metal at 700K. The $\text{TaCl}_5(\text{g})$ was mixed with hydrogen down stream from the chlorinator and then introduced into the deposition chamber. For experiments involving coating of the graphite cloth with Ta-C alloys, propylene, $\text{C}_3\text{H}_6(\text{g})$, was added to the hydrogen. In some experiments $\text{HCl}(\text{g})$ was added to the hydrogen in order to prevent gas phase nucleation from occurring. All gas flows were controlled using calibrated flow controllers or flow meters.

The metal deposition chamber was heated by radiation from a 36 in. long Lindberg clamshell resistance furnace which contained three independently controlled temperature zones. Type K thermocouples were used throughout the system to measure all

pertinent temperatures.

Figure 1 shows a schematic diagram of the CVD apparatus. Figure 2 shows details of the coating chamber.

V. Results of the Thermodynamic Calculations

A. The Ta-Cl-H System

The computed CVD phase diagram for this three component system between 700K and 1300K for H/Cl ratios in the input gas between 0 and 18 is shown in Figure 3. The phase diagram is dominated by the Ta(s) single phase region above approximately 800K for H/Cl > 6 and by the TaCl_{2.5}(s) single phase region below 800K. For H/Cl < 6 the minimum temperature at which single phase Ta(s) may be deposited increases as H/Cl decreases while the maximum temperature at which single phase TaCl_{2.5}(s) deposits decreases as H/Cl decreases. For H/Cl > 6, a very narrow Ta(s) + TaCl_{2.5}(s) two phase region (i.e. the region in which Ta(s) and TaCl_{2.5}(s) co-deposit) separates the Ta(s) and TaCl_{2.5}(s) single phase regions. For H/Cl < 6, a region in which no solid phase may deposit separates the Ta(s) and TaCl_{2.5}(s) single phase regions. Thus for H/Cl = 2.5, TaCl_{2.5}(s) deposits below 750K and Ta(s) deposits above approximately 900K.

Figure 4 shows the calculated equilibrium vapor composition as a function of H/Cl in the input gas for the Ta-Cl-H system at 1025K and a total system pressure of 0.03 atm. The predominant Ta-containing vapor species is seen to be TaCl₄(g). The vapor pressure of TaCl₅(g) is about a factor of 10 lower than that for TaCl₄(g) and the vapor pressure of TaCl₃(g) is about a factor of 100 lower than that for TaCl₄(g). All other vapor species not shown in the Figure were calculated to have equilibrium pressures below 1×10^{-6} atm. at 1025K.

It is seen in Figure 4 that as the H/Cl ratio in the input gas increases (i.e. as more H₂ is added to the input gas) the Ta-containing vapor species decrease in pressure. This behavior must correspond to additional Ta(s) deposition as the H/Cl ratio increases. This is shown in Figure 5 where the amount of Ta(s) deposited as a function of H/Cl in the input gas is shown as the solid curve for three deposition temperatures- 1025K,

1125K, and 1225K. The curves for 1025K and 1125K were computed using a total of 0.18 moles of tantalum in the system while the curve for 1225K was computed using a total of 0.3 moles of tantalum. The three circles in Figure 5 represent experimental results of three CVD experiments in which Ta metal was deposited on graphite cloth. These results and the process parameters for the experiments are summarized in Table 2. A fourth experiment (Expt. 2) listed in Table 2, for which $H/Cl = 15.2$, is not shown in Figure 5. Comparison of the actual amount of Ta(s) deposited on the graphite cloth in the three CVD experiments with the calculated maximum amount of Ta(s) which could be deposited under the conditions of the experiment gives deposition efficiencies of 58.6%, 34.1%, and 52.0% at 1025K, 1125K, and 1225K respectively.

B. The Ta-C-Cl-H System.

Experimentally, the only major difference between this four component system and the Ta-Cl-H system was that propylene, $C_3H_6(g)$, was added to the input gas to provide a source of carbon. The input gases were mixed in the baffle region of the CVD apparatus above the deposition chamber at an approximate temperature of 500K. If during this mixing the gas achieved thermodynamic equilibrium, the $C_3H_6(g)$ would be almost completely converted to methane. Figure 6 shows the calculated equilibrium composition as a function of Ta/C for the input gas at 500K, $P_T = 0.03$ atm., and $H/Cl = 2$. As seen in the Figure, $CH_4(g)$ is the only important C- containing vapor species in the equilibrium input gas. Also, $TaCl_5(g)$ is the only important Ta- containing vapor species in the equilibrium input gas.

Figure 7 shows the calculated equilibrium CVD phase diagram for the Ta-C-Cl-H system between 700K and 1225K as a function of Ta/C in the input gas at constant values of $H/Cl = 10.8$ and $P_T = 0.03$ atm.. The region of the phase diagram above Ta/C = 2.5 was not calculated in this work. The distinguishing features of this phase diagram are that the TaC(s) single phase region is very narrow above 1000K and broadens over a wide temperature range as the deposition temperature decreases, and that the $Ta_2C(s)$ single phase region is very narrow above 1200K and broadens towards Ta/C values greater than 2 as the deposition temperature decreases.

It should be noted that we assumed TaC(s) to be stoichiometric throughout these calculations (e. g. the homogeneity range over which TaC exists was ignored). The effect of taking into account the homogeneity range of TaC would be to broaden the TaC(s) single phase region of the phase diagram over Ta/C values greater than 1.

Figure 8 shows the effect on the phase diagram of reducing the H/Cl ratio for the input gas. The TaC(s) single phase region is seen to broaden towards higher Ta/C values and the maximum deposition temperature for single phase TaC(s) decreases for Ta/C < 1 and increases for Ta/C > 1.

Figures 9 and 10 show the calculated equilibrium gas phase composition for the Ta-C-Cl-H system at 1200K, $P_T = 0.03$ atm. for values of Ta/C between 0.1 and 2.5. Figure 9 is for H/Cl = 10.7 and Figure 10 is for H/Cl = 2. In both cases $CH_4(g)$ is the major C-containing molecule above the C+TaC two phase region and its equilibrium concentration decreases towards the more Ta-rich portion of the phase diagram. $TaCl_4(g)$, $TaCl_3(g)$ and $TaCl_5(g)$ are calculated to be the important Ta-containing gaseous molecules and their equilibrium concentrations increase towards the more Ta-rich portion of the phase diagram. Note also that the vapor composition is fixed across the C+TaC, TaC+Ta₂C, and Ta+Ta₂C two phase regions; that the equilibrium vapor pressures for the Ta-containing molecules increase as H/Cl decreases; and that the equilibrium vapor pressures for the C-containing molecules decrease as H/Cl decreases.

Process parameters for Ta-C alloy deposition on graphite cloth, observed phases, and phases predicted to be deposited using the CVD phase diagram in Figure 8 are given in Table 3. The observed phases were determined from their X-ray diffraction patterns. Lattice parameters were calculated for the TaC phases from the back-reflection lines of the X-ray diffraction patterns. The composition of the TaC phases as derived from the calculated lattice parameters³² was $TaC_{0.82}$ for all TaC-containing deposits investigated.

The TaC deposited on the graphite cloths in Expt. 33 was observed to be a fine, powdery material indicating that gas phase nucleation had occurred during the experiment. Accordingly, HCl(g) was added to the input gas of Expts. 38 through 41 in order to depress the occurrence of gas phase nucleation.

Expts. 40 and 41 used HCl(g) flow rates which were twice the flow rates used in Expts. 38 and 39. As seen in Table 3, holding all other process parameters constant

but doubling the HCl(g) flow rate causes the deposited material to change from $\text{Ta}_2\text{C(s)}$ to TaC(s) .

VI. Discussion

A. The Ta-Cl-H System

The CVD of tantalum metal using $\text{TaCl}_5(\text{g})$ as the reactant gas can take place in a hydrogen atmosphere at temperatures as low as 775K to 800K if the H/Cl ratio in the input gas is greater than 6. It would appear that co-deposition of Ta(s) and $\text{TaCl}_{2.5}(\text{s})$ would be experimentally difficult in view of the very narrow (5° to 10°) temperature region over which the two phases co-exist.

B. The Ta-C-Cl-H System

Process conditions for which a particular Ta-C alloy may deposit as predicted from the equilibrium CVD phase diagram for the Ta-C-Cl-H system are not in accord with results obtained experimentally in our CVD apparatus using woven graphite cloths as a substrate. In all cases, the actual vapor deposited material appears to be richer in tantalum than would be predicted from the CVD phase diagram. For example, under the process conditions for Expt. 38 the phase diagram predicts the deposit to be two phase TaC and C while the actual deposit is observed to be Ta_2C . In Expt. No. 41 the phase diagram predicts two phase TaC and C as the deposit while the actual deposit was observed to be TaC (All TaC deposits had a composition of $\text{TaC}_{0.82}$. We believe this to be the lower TaC phase boundary composition at 1225K as determined by extrapolation of the estimated lower TaC phase boundary¹³ from 1773K to 1225K). Also, freely deposited carbon was never observed in any of the deposited material analyzed by X-ray diffraction.

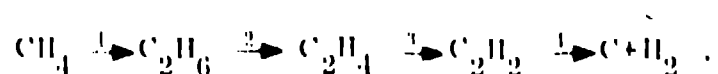
There are few experimental details and results of investigations reported in the literature involving the CVD of Ta-C alloys with which we can compare the results of our experiments and thermodynamic calculations. Early CVD experiments involved the preparation of TaC at temperatures greater than 2300K using $\text{TaCl}_5(\text{g})$ and methane,

acetylene, or toluene as the reactant gases.⁵¹ Ambartsumyan and Babich⁵² prepared TaC by thermal dissociation of $\text{TaCl}_5(\text{g})$ on graphite substrates at temperatures between 2323K and 2813K and found stoichiometric TaC in contact with the graphite substrate and $\text{TaC}_{0.89}$ on the outer layer of the deposit. Crayton and Gridly⁵³ prepared submicron TaC powder by the vapor phase reaction of methane and $\text{TaCl}_5(\text{g})$ between 1673K and 1873K. Takahashi and Sugiyama⁵⁴ used an A-C discharge method to grow TaC fibers from $\text{TaCl}_5(\text{g})$ and propylene reactant gases at temperatures between 523K and 923K. Grossklauss and Bunshah⁵⁵ deposited TaC and Ta_2C on either 302 stainless steel or molybdenum substrates between 823K and 1763K by vaporizing tantalum metal in the presence of acetylene.

Heffernan, Ahmad and Haskell⁵⁶ used CVD to prepare Ta-C alloys on a resistively heated tungsten filament at 1373K using $\text{TaCl}_5(\text{g})$ and methane as reactant gases. The results of their experiments are summarized in Table 4 along with the Ta-C phases predicted from the CVD phase diagram. As can be seen from the table, the observed Ta-C phases are Ta-rich compared to the predicted phases as observed in our work.

The results of Heffernan, Ahmad and Haskell along with the results of the present work causes us to believe that a kinetically limiting step in the pyrolysis of $\text{C}_3\text{H}_4(\text{g})$ (or of $\text{C}_3\text{H}_6(\text{g})$ in the present work) either in the gas phase or on the substrate surface may be the cause for the Ta-C deposits to be deficient in carbon. Unfortunately, virtually nothing is known about the kinetics and mechanism of the chemical processes occurring in CVD experiments such as those performed in the present work. However, we can gain a rough idea as to whether a kinetically limiting step in the pyrolysis of methane would be a reasonable factor in forming carbon deficient Ta-C alloys in our CVD experiments.

The kinetics and mechanisms of $\text{CH}_4(\text{g})$ pyrolysis to form C(s) have been previously reviewed.⁵⁷ It has been postulated that carbon(s) formed by a series of consecutive first order reactions as follows:



Step 1 was postulated to be rate-controlling below 1800K while step 4 was postulated to

be rate-controlling above this temperature. The first order rate constant for the rate-controlling step, reaction 1, is well established and is:⁵³⁻⁶⁰

$$k_1 = 10^{14.58} \exp(-103,000/RT) \text{ sec}^{-1} . \quad (1)$$

Equation 1 was used to calculate the amount of carbon formed at 1225K and the results were then compared with the amount of tantalum metal deposited in our experiments with the Ta-Cl-H system. The results of the calculations showed that the formation of C-deficient Ta-C alloys could be qualitatively explained by the pyrolysis of methane being rate-controlled by reaction 1. In light of this result, it would be instructive to perform some experiments in which an appropriate catalyst was added to the Ta-C-Cl-H input gas stream or placed on the graphite cloth surface to try to enhance the carbon deposition rate.

Another problem which is not clearly understood is the strong effect that the concentration of HCl(g) in the input gas has on determining the composition of the Ta-C alloy deposits. This behavior may indicate a large local buildup of HCl(g) among the fibers of the graphite cloth causing a shift in the equilibrium $2H_2(g) + TaCl_4(g) \rightleftharpoons Ta(s) + 4HCl(g)$ to the left.

References

1. M. F. Smith, Chemical Vapor Deposition, Vol. 1, 1964-1974 (A Bibliography with Abstracts), National Technical Information Service report NTIS/PS-76/0521, 1976.
2. M. F. Smith, Chemical Vapor Deposition, Vol. 2, 1975-July, 1977 (A Bibliography with Abstracts), National Technical Information Service report NTIS/PS-77/0613, 1977.
3. A. C. Schaffhauser, Ed., Chemical Vapor Deposition of Refractory Metals, Proc. of Gatlinburg, Tenn., Conf., Sept., 1967, Amer. Nucl. Soc., Hinsdale, Ill., 1967.
4. J. M. Blocher, Jr. and J. C. Withers, Eds., Chemical Vapor Deposition, Proc. Second Int. Conf., Los Angeles, May, 1970, The Electrochem. Soc., Princeton, NJ, 1970.
5. F. A. Glaski, Ed., Chemical Vapor Deposition, Proc. Third Int. Conf., Salt Lake City, April, 1972, Amer. Nucl. Soc., Hinsdale, Ill., 1972.
6. G. F. Wakefield and J. M. Blocher, Jr., Eds., Chemical Vapor Deposition, Proc. Fourth Int. Conf., Oct., 1973, The Electrochem. Soc., Princeton, NJ, 1973.
7. J. M. Blocher, Jr., H. E. Hinterman and I. H. Hall, Eds., Chemical Vapor Deposition, Proc. Fifth Int. Conf., Fulmer Grange, England, Sept., 1975, The Electrochem. Soc., Princeton, NJ, 1975.
8. L. F. Donaghey, P. Rat-Choudhury and R. N. Tauher, Eds., Chemical Vapor Deposition, Proc. Sixth Int. Conf., Atlanta, Oct., 1977, The Electrochem. Soc., Princeton, NJ, 1977.
9. T. O. Sedgwick and H. L. Johnston, Eds., Chemical Vapor Deposition, Proc. Seventh Int. Conf., Los Angeles, Oct., 1979, The Electrochem. Soc., Princeton, NJ, 1979.
10. L. R. Newkirk, F. A. Valencia and T. C. Wallace "The Preparation of High T_c Nb₃Ge Superconductors by Chemical Vapor Deposition", pp. 704-712, Ref. 7.
11. L. R. Newkirk and F. A. Valencia "Method for Preparing High-Transition-Temperature Nb₃Ge Superconductors", U. S. Patent 4,054,686, Oct. 18, 1977.
12. A. Reisman and T. O. Sedgwick "Chemical Vapor Deposition and Solid-Vapor Equilibria" In Phase Diagrams: Materials Science and Technology, Vol. IV, A. M. Alper, Ed., pp. 1-90, Academic Press, NY, 1976.
13. J. J. Cuomo, J. F. Ziegler and J. M. Woodwal "A New Concept for Solar Energy Conversion" Appl. Phys. Lett., 26, 557(1975).
14. D. P. Grimmer, K. C. Herr and W. J. McCreary "Possible Selective Solar Photothermal Absorber: Ni Dendrites on Al Surfaces by the CVD of Ni(CO)₄", J. Vac. Sci. Technol., 15, 59(1978).
15. J. J. Nickl, K. K. Schweitzer and P. Luxenberg "Chemical Vapor Deposition of the Systems Ti-Si-C and Ti-Ge-C", pp. 4-23, Ref. 5.

16. J. Buehler, E. Fitzer and D. Kehr "Chemical Vapor Deposition of Silicon Nitride", pp. 493-496, Ref. 8.
17. H. O. Pierson, E. Randich and A. W. Mullendore "Chemical Vapor Deposition of Transition Metal Borides", following paper at this Conference.
18. H. O. Pierson and E. Randich "The Coating of Metals with Titanium Diboride by Chemical Vapor Deposition", pp. 304-317, Ref. 8.
19. M. G. Bowman and D. T. Vier "Gas Mixture for Forming Protective Coatings on Graphite", U. S. Patent 3,785,994, January 15, 1974.
20. T. C. Wallace, Sr. "Chemical Vapor Deposition of ZrC in Small-Bore Carbon-Composite Tubes", pp. 91-106, Ref. 6.
21. T. C. Wallace, Sr. and M. G. Bowman "Chemical Vapor Deposition: A Technique for Applying Protective Coatings", invited paper presented at the DoE-EMACC Conference, Argonne National Laboratory, Argonne, Ill., June, 1979. Los Alamos Scientific Laboratory report LA-UR-79-1470.
22. T. C. Wallace, Sr., G. E. Cort, J. J. Damman and M. C. Cline "Development of Pyrolytic Graphite/Silicon Carbide Composite Materials for Rocket-Nozzle Applications, Vol. I, The Injector Deposition Furnace", Los Alamos Scientific Laboratory report LA-UR-77-2444 (Oct., 1977).
23. T. C. Wallace, Sr., G. E. Cort, J. J. Damman, D. B. Court, D. E. Hull and R. W. Meier "Development of Pyrolytic Graphite/Silicon Carbide Composite Materials for Rocket-Nozzle Applications, Vol. II, The Channel Flow Furnace", Los Alamos Scientific Laboratory report LA-UR-77-2042 (Sept., 1977).
24. G. E. Cort, J. J. Damman and T. C. Wallace, Sr. "Development of Pyrolytic Graphite/Silicon Carbide Composite Materials for Rocket-Nozzle Applications, Vol. III, Comparison of Deposition Furnaces and a Generic Process Control System Specifications", Los Alamos Scientific Laboratory report LA-UR-77-2679 (Nov., 1977).
25. T. C. Wallace, Sr. "Development of a Process Control Model for the Application of Co-Deposited Materials" paper presented at the Air Force Materials Laboratory Technical Conf. on Analysis and Fabrication of Carbon/Carbon (Involute) Exit Cones, Feb. 21-22, 1979, Bergamo Conference Center, Dayton, OH.
26. R. E. Riley and T. C. Wallace, Sr. "Method for Making Hot-Pressed Fiber-Reinforced Carbide-Graphite Composite", U. S. Patent 4,180,428, Dec. 25, 1979.
27. C. M. Hollabaugh, K. V. Davidson, C. L. Radosevich, R. E. Riley and T. C. Wallace, Sr. "Chemical Vapor Deposition of Tantalum on Graphite Cloth for Making Hot-Pressed Fiber-Reinforced Carbide-Graphite Composite", pp. 559-573, Ref. 8.
28. L. R. Newkirk, R. E. Riley, H. Shelnberg, F. A. Valencic and T. C. Wallace, Sr. "Preparation of Unidirectional Fiber Reinforced Tantalum Carbide Composites", pp. 488-498, Ref. 9.
29. L. R. Newkirk, R. E. Riley, H. Shelnberg, F. A. Valencic and T. C. Wallace, Sr.

- "Preparation of Fiber Reinforced Titanium Diboride and Boron Carbide Composite Bodies", pp. 515-524, Ref. 9.
30. R. E. Riley, T. C. Wallace, Sr. and J. M. Dickinson "Composite Materials for Tokamak Wall Armor, Limiters, and Beam Dump Applications", J. Nucl. Mater. 85-86, 221(1979).
 31. T. M. Besmann "SOLGASMIX-PV, a Computer Program to Calculate Equilibrium Relationships in Complex Chemical Systems", Oak Ridge National Laboratory report ORNL/TM-5775 (April, 1977).
 32. E. K. Storms, The Refractory Carbides, Academic Press, NY, 1967.
 33. L. E. Toth, Transition Metal Carbides and Nitrides, Academic Press, NY, 1971.
 34. H. L. Schick, Thermodynamics of Certain Refractory Compounds, Vols. I and II, Academic Press, NY, 1966.
 35. Ya. I. Gerassimov and V. I. Lavrentev, Tantalum. Physicochemical Properties of Its Compounds and Alloys. Thermochemical Properties. At. Energy Rev. (Spec. Issue 3), pp. 7-39, 1972.
 36. H. Schaefer, H. Scholz and R. Gerken, "The Chemistry of Niobium and Tantalum. XXXV. The Lower Chlorides of Tantalum", Z. anorg. allg. Chem. 331, 154(1964).
 37. M. W. Chase, Jr., J. L. Curnutt, R. A. McDonald and A. N. Syverud, J. Phys. Chem. Ref. Data 7, 89(1978).
 38. R. C. Feber, Los Alamos Scientific Laboratory, unpublished results.
 39. H. Schaefer and F. Kahlenberg, "The Heat of Formation of Tantalum (IV) Chloride and the Thermochemistry of the Chlorides $TaCl_5$, $TaCl_4$ and $TaCl_3$ ", Z. anorg. allg. Chem. 305, 178(1960).
 40. I. Barin and O. Knacke, Thermochemical Properties of Inorganic Substances, Springer-Verlag, Berlin, 1973.
 41. R. G. Behrens and R. C. Feber "Thermodynamic Properties of Gaseous Tantalum-Chlorine Molecules", submitted to J. Less-Common Metals.
 42. D. R. Stull and H. Prophet, JANAF Thermochemical Tables, Second Ed., Nat. Stand. Ref. Data Ser., Nat. Bur. Stand. (U.S.) publication NSRDS-NBS-37; June, 1971.
 43. D. R. Stull, E. F. Westrum, Jr. and G. C. Sinke, The Chemical Thermodynamics of Organic compounds, John Wiley and Sons, Inc., NY, 1969.
 44. R. Hultgren, P. D. Desai, D. T. Hawkins, M. Gleiser, K. K. Kelley, and D. D. Wagman, Selected Values of the Thermodynamic Properties of the Elements, Am. Soc. Metals, Metals Park, OH, 1973.
 45. G. Eriksson "Thermodynamic Studies of High Temperature Equilibria. III. SOLGAS, a Computer Code for Calculating the Composition and Heat Conditions of an Equilibrium

- Mixture", *Acta Chem. Scand.* 25, 2651(1971).
46. G. Eriksson and E. Rosen "Thermodynamic Studies of High Temperature Equilibria. VIII. General Equations for the Calculation of Equilibria in Multiphase Systems", *Chem. Scripta* 4, 193(1973).
 47. G. Eriksson "Thermodynamic Studies of High Temperature Equilibria. XII. SOLGASMIX, a Computer Program for Calculation of Equilibrium Compositions in Multiphase Systems", *Chem. Scripta* 8, 100(1975).
 48. C. F. Wan and K. E. Spear "Thermodynamic Equilibrium in the Nb-Ge-H-Cl System for the Chemical Vapor Deposition of Nb₃Ge", pp. 47-58, Ref. 8.
 49. K. E. Spear "Application of Phase Diagrams and Thermodynamics to CVD", pp. 1-16, Ref. 9.
 50. T. M. Besmann and K. E. Spear "Analysis of the Chemical Vapor Deposition of Titanium Diboride. I. Equilibrium Thermodynamic Analysis", *J. Electrochem. Soc.* 124, 786(1977).
 51. K. Becker and H. Ewest "Die physikalischen und Strahlungstechnischen Eigenschaften des Tantalcarbides", *Z. techn. Physik.* 11, 148(1930).
 52. R. S. Ambartsumyan and B. N. Babich "Formation of Niobium and Tantalum Carbides by Thermal Dissociation of the Chlorides on a Graphite Substrate", *izvet. Akad. Nauk, SSSR, Inorganic Mat.* 6, 1074(1970).
 53. P. H. Crayton and M. C. Gridly "Vapour-Phase Synthesis of Submicron Tantalum Carbide", *Powder Met.* 14, 78(1971).
 54. T. Takahashi and K. Sugiyama "Fibrous Growth of Tantalum Carbide by A-C Discharge Method", *J. Electrochem. Soc.* 121, 714(1974).
 55. W. Grossklauss and R. F. Bunshah "Synthesis and Morphology of Various Carbides in the Ta-C System", *J. Vac. Sci. Technol.* 12, 811(1975).
 56. W. J. Heffernan, I. Ahmad and R. W. Haskell "A Continuous CVD Process for Coating Filaments with Tantalum Carbide", pp. 498-508, Ref. 6.
 57. W. V. Kottensky "Deposition of Pyrolytic Carbon in Porous Solids", in *Chemistry and Physics of Carbon*, Vol. 9; P. L. Walker and P. A. Thrower, Eds.; pp. 173-259, Marcel Dekker, Inc., NY, 1973.
 58. H. B. Palmer and T. J. Hart "The Activation Energy for the Pyrolysis of Methane", *J. Phys. Chem.* 67, 709(1963).
 59. D. W. Placzek, B. S. Rabinovitch and G. Z. Whitten "Some Comparisons of the Classical RRK and the RRKM Theoretical Rate Formulations", *J. Chem. Phys.* 43, 407(1965).
 60. I. G. Murgulescu and Z. Simon "Calculations of Preexponential Coefficients of Unimolecular Reactions", *Acad. Rep. Populare Romine, Studii Cercetari Chim* 10, 11(1962).

Table 1. Thermochemical Data Used to Prepare Input for Complex Equilibrium Calculations of the Ta-Cl-H and Ta-C-Cl-H Systems.

$\Delta H_f^0(298.15K)$ (kcal mol ⁻¹)		$-[G^0(T) - H^0(298.15K)]/T$ (cal K ⁻¹ mol ⁻¹)							
		500K	700K	900K	900K	1000K	1100K	1200K	1300K
Gaseous Molecules:									
H ₂	0.0	32.00	33.15	33.72	34.25	34.76	35.24	35.70	36.13
Cl ₂	0.0	54.23	55.64	56.33	57.00	57.62	58.22	58.78	59.32
HCl	-22.06	45.44	46.60	47.16	47.70	48.22	48.71	49.18	49.62
TaCl ₅	-132.80	101.74	106.77	109.22	111.57	113.79	115.90	117.90	119.79
TaCl ₄	-137.09	92.39	96.99	98.99	100.90	102.71	104.43	106.05	107.59
TaCl ₃	-77.0	84.76	87.90	89.43	90.90	92.29	93.60	94.85	96.03
TaCl ₂	-16.0	72.83	75.25	76.40	77.50	78.55	79.54	80.48	81.37
TaCl	86.0	62.90	64.34	65.04	65.71	66.34	66.94	67.51	68.05
CH ₄	-17.9	45.53	47.26	48.18	49.10	50.02	50.92	51.81	52.69
C ₂ H ₂	51.19	49.30	51.38	52.43	53.46	54.47	55.43	56.37	57.27
C ₂ H ₄	14.58	53.72	56.00	57.22	58.45	59.67	60.87	62.04	63.20
C ₃ H ₆	4.88	65.80	69.24	71.09	72.96	74.81	76.64	78.45	80.24
C ₆ H ₆	19.82	67.05	71.93	74.60	77.29	79.98	82.67	85.33	88.05
CCl ₄	-22.42	76.42	80.12	81.97	83.74	85.44	87.06	88.60	90.06
C ₂ H ₆	-20.24	56.49	59.33	60.86	62.42	63.96	65.50	67.00	68.48
CH ₃ Cl	-18.76	57.21	59.25	60.32	61.39	62.45	63.49	64.50	65.49
CH ₂ Cl ₂	-21.19	66.10	68.58	69.87	71.14	72.38	73.58	74.74	75.87
CHCl ₃	-23.49	72.55	75.59	77.14	78.64	80.10	81.49	82.83	84.12

Table 1. Continued

Solid Phases:

Ta	0.0	10.62	11.65	12.16	12.64	13.10	13.53	13.95	14.34
TaCl ₅	-205.3	57.01	62.89	65.82	68.76	71.70	74.64	77.58	80.52
TaCl ₄	-169.1	49.35	54.38	56.94	59.53	62.15	64.80	67.43	70.19
TaCl ₃	-132.2	39.61	43.56	45.51	47.39	49.18	50.79	52.76	54.55
Ta ₂ Cl ₅	-226.8	71.78	78.58	81.90	85.08	88.08	90.90	93.54	96.00
C	0.0	1.42	2.17	2.45	2.74	3.02	3.30	3.57	3.84
TaC _{1.0}	-34.09	11.20	12.92	13.79	14.64	15.46	16.24	16.99	17.72
Ta ₂ C	-47.27	21.25	23.94	25.28	26.58	27.82	29.02	30.16	31.25

Table 2. Experimental Parameters and Results for the CVD of Tantalum Metal on Graphite Cloth.

<u>Expt.</u>	<u>Flow Rates</u> <u>[cm³(STP) s⁻¹]</u>			<u>Moles Ar</u> <u>Input Gas</u>	<u>Moles H₂ / Moles Cl₂</u> <u>Input Gas</u>	<u>Temp.</u> <u>(K)</u>	<u>Comment</u>
	<u>Ar</u>	<u>H₂</u>	<u>Cl₂</u>				
2	173	1500	99	4.2	15.2	1115	16.6 g Ta deposited
15	173	400	57	2.1	7.0	1225	23.5 g Ta deposited
21	179	650	61	1.4	10.4	1025	13.8 g Ta deposited
23	179	650	61	1.4	10.6	1125	10.5 g Ta deposited

Table 3. Summary of Experimental Results for the CVD of Ta-C Alloys on Graphite Cloth.

Expt.	Temp. (K)	Moles H ₂ /Moles Cl (Input Gas)	Moles Ta/Moles C (Input Gas)	Phases Predicted	Phases Observed
31	1125	10.7	1	TaC	~ (90% Ta + 10% Ta ₂ C)
32	1225	10.8	1	TaC	~ (60% Ta + 40% Ta ₂ C)
33	1225	4.3	0.4	TaC+C	TaC+Gas Phase Nucleation
35*	1225	4.6	0.4	TaC+C	Ta ₂ C
39*	1225	2.5	0.4	TaC+C	Ta ₂ C
40*	1225	2.2	0.4	TaC+C	TaC
41*	1225	2.4	0.3	TaC+C	TaC

* HCl added to input gas

Table 4. Summary of Results for the CVD of Ta-C Alloys on Tungsten Wire (Heffernan, Ahmad and Haskell)*

Moles Ta/Moles C (Input Gas)	Phases Predicted	Phases Observed
1.6	TaC, Ta ₂ C	Ta ₂ C, trace- Ta
0.4	TaC, C	TaC, Ta ₂ C, trace-Ta
0.27	TaC, C	TaC, trace-Ta ₂ C
0.20	TaC, C	TaC, trace-Ta ₂ C
0.04	TaC, C	TaC

* Experiments performed at 1373K using HCl in the chlorinator and CH₄(g) as the carbon source.

Figure Captions

- Figure 1. Schematic diagram of CVD apparatus for coating woven graphite cloth with Ta-C alloys. Arrows indicate direction of gas flow.
- Figure 2. Schematic diagram showing details of deposition chamber.
- Figure 3. Calculated equilibrium CVD phase diagram for the Ta-Cl-H system.
 $P_T = 0.03 \text{ atm.}$
- Figure 4. Calculated equilibrium vapor composition for the Ta-Cl-H system.
at $P_T = 0.03 \text{ atm.}$ and $T = 1025\text{K.}$
- Figure 5. Comparison of maximum amount of tantalum metal capable of being deposited in the Ta-Cl-H system (solid curves) with amounts actually found deposited for three CVD experiments using woven graphite cloth as a substrate. $P_T = 0.03 \text{ atm.}$ $T = 1025\text{K, } 1125\text{K, and } 1225\text{K.}$ Open circles represent data points.
- Figure 6. Computed equilibrium vapor composition of the input gas for CVD experiments in the Ta-C-Cl-H system. $P_T = 0.03 \text{ atm., } T = 500\text{K.}$
 $\text{H/Cl} = 2.$
- Figure 7. Computed equilibrium CVD phase diagram for the Ta-C-Cl-H system.
 $\text{H/Cl} = 10.8, P_T = 0.03 \text{ atm.}$
- Figure 8. Computed equilibrium CVD phase diagram for the Ta-C-Cl-H system.
 $\text{H/Cl} = 2, P_T = 0.03 \text{ atm.}$
- Figure 9. Equilibrium vapor composition for the Ta-C-Cl-H system at 1200K.
 $P_T = 0.03 \text{ atm., } \text{H/Cl} = 10.7.$
- Figure 10. Equilibrium vapor composition for the Ta-C-Cl-H system at 1200K.
 $P_T = 0.03 \text{ atm., } \text{H/Cl} = 2.$

FIGURE 1

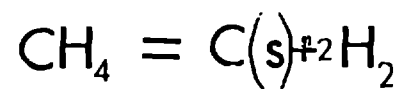
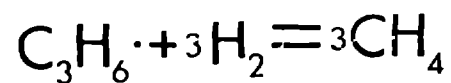
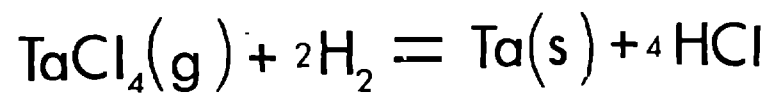
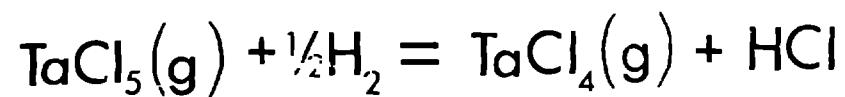
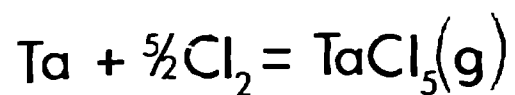
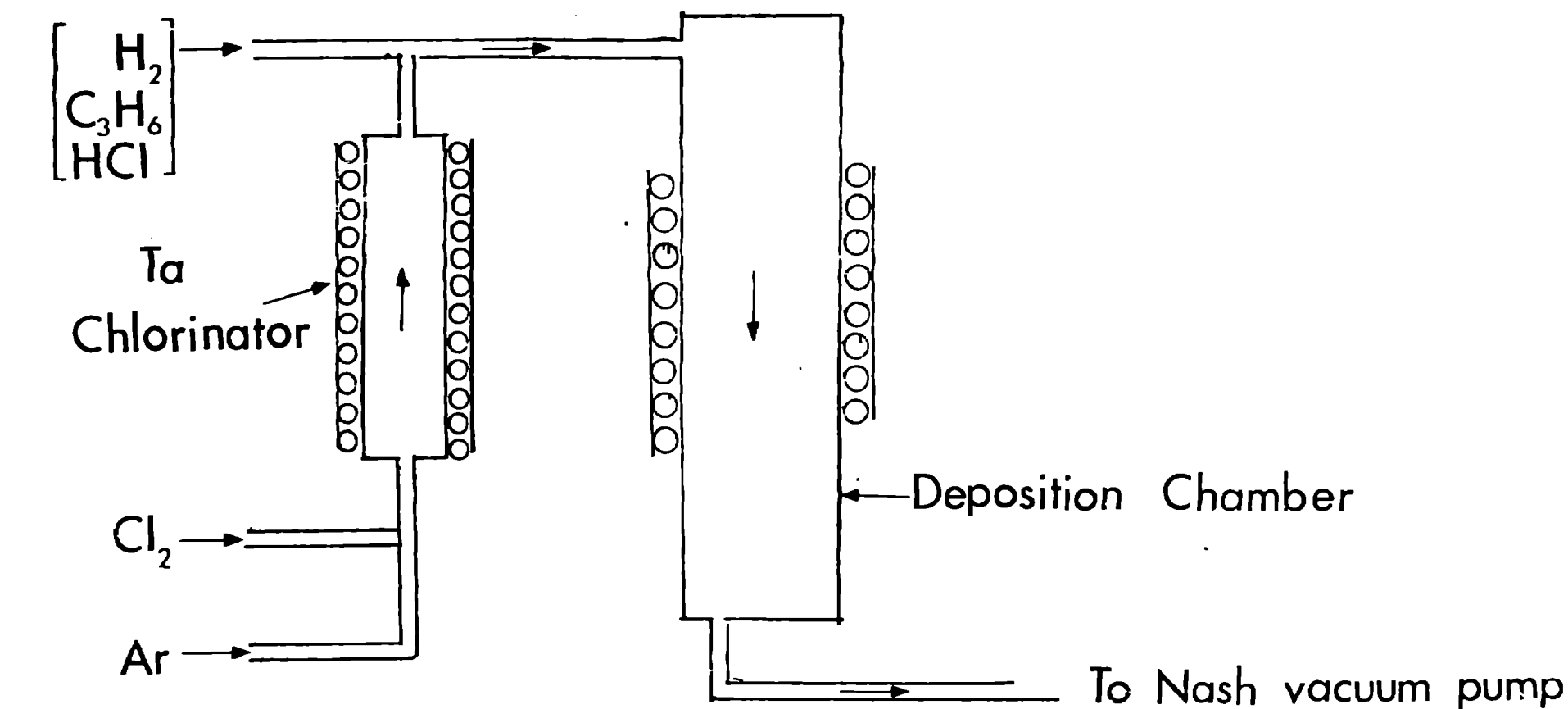


FIGURE 2

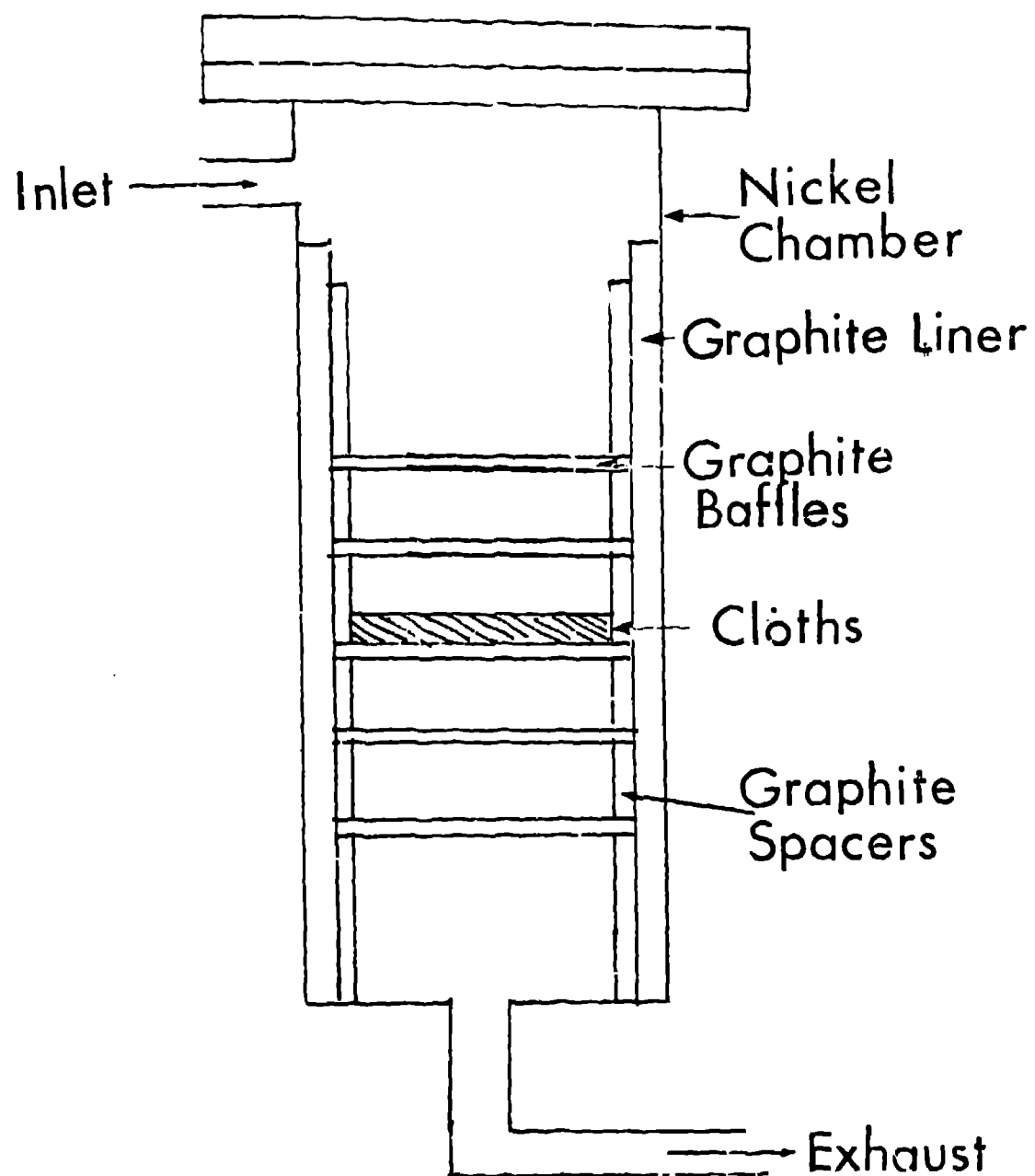
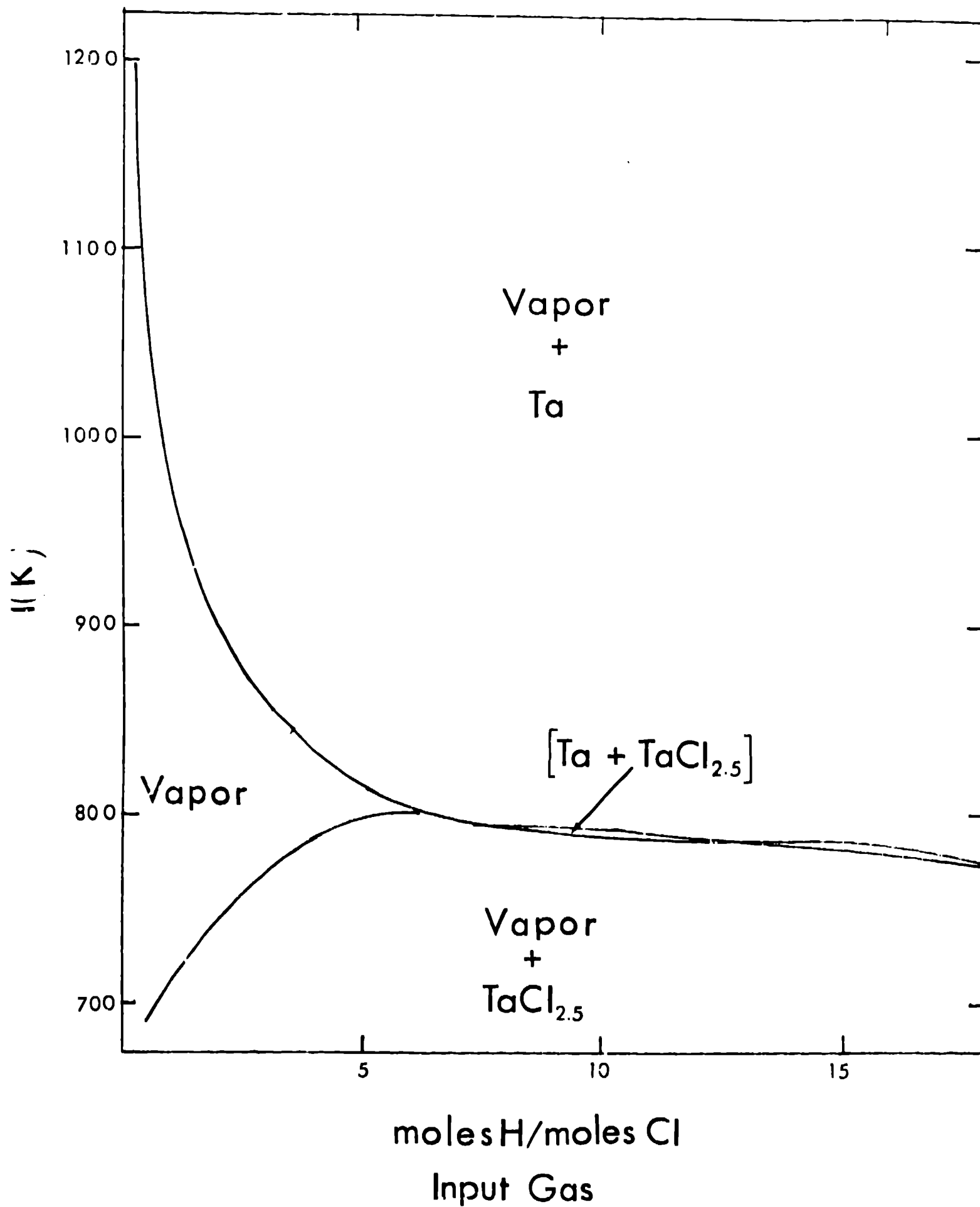


FIGURE 3



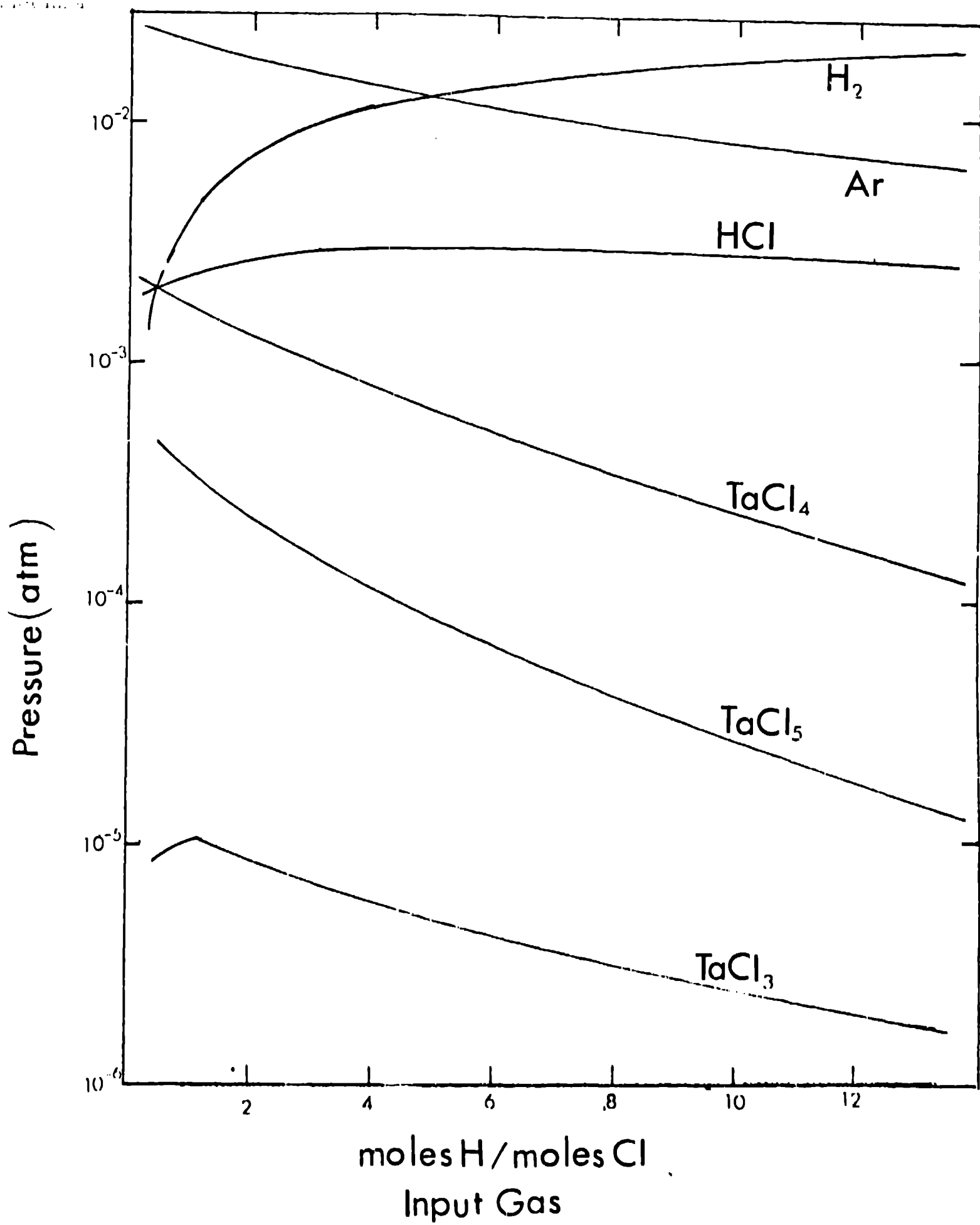


FIGURE 5

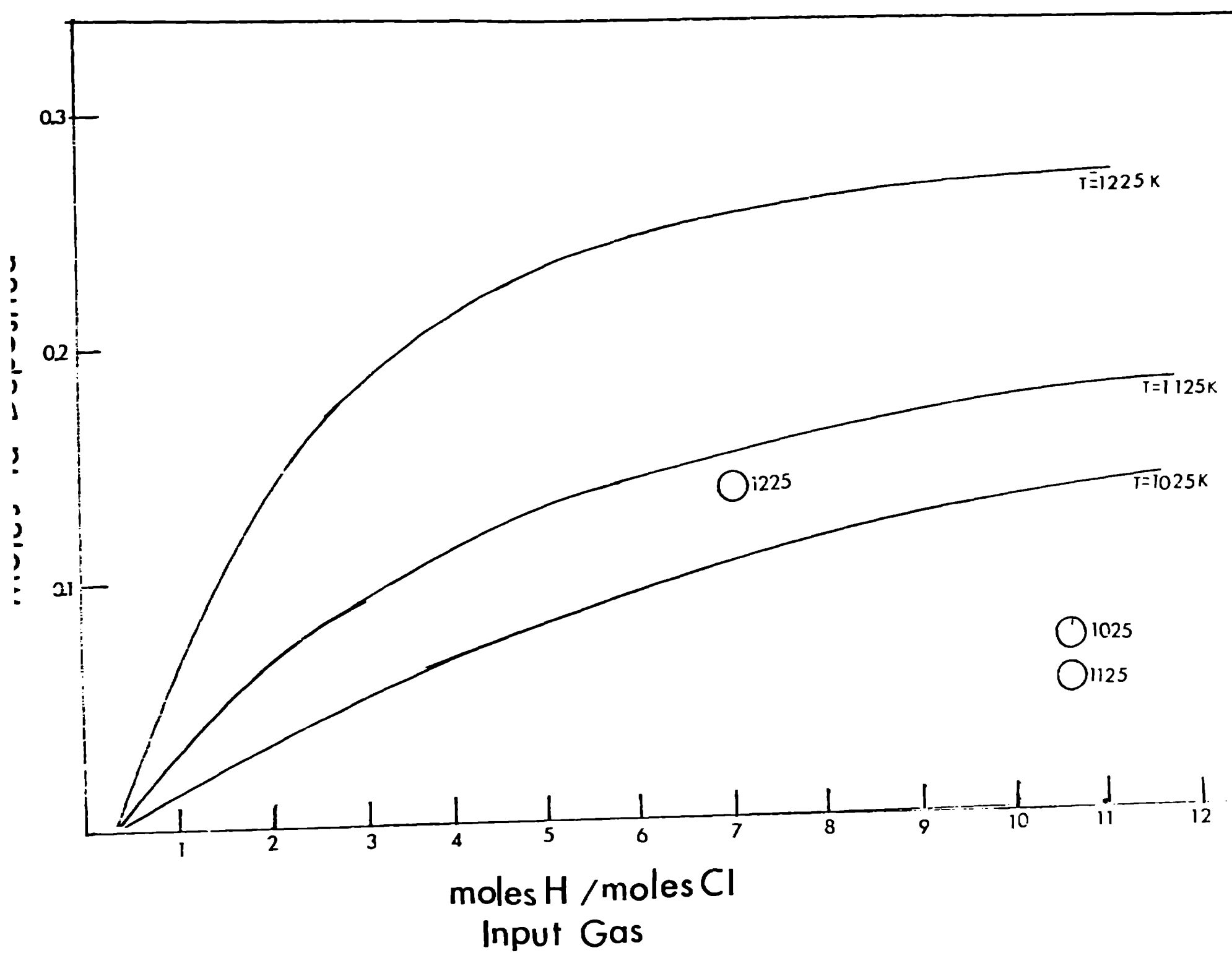


FIGURE 6

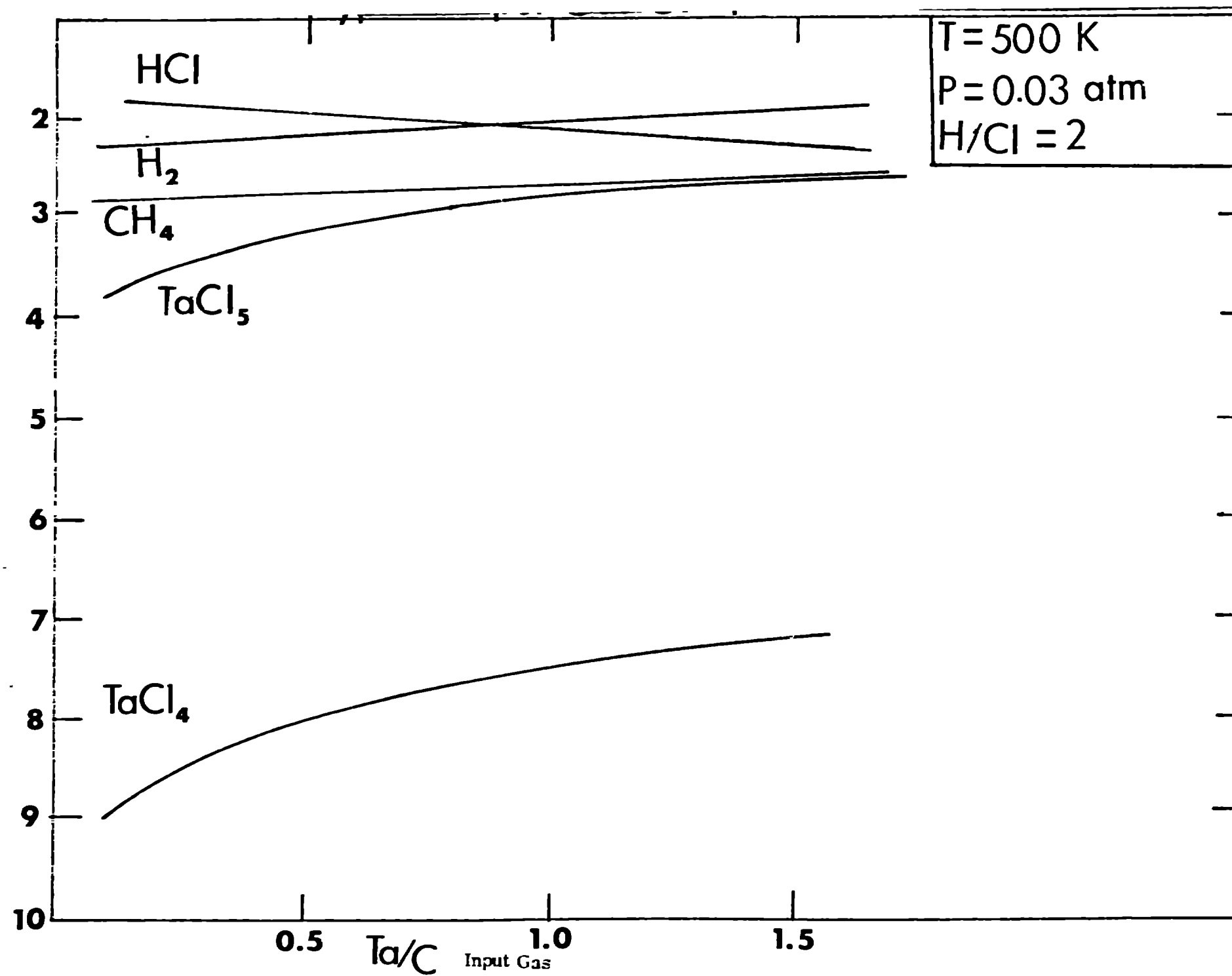
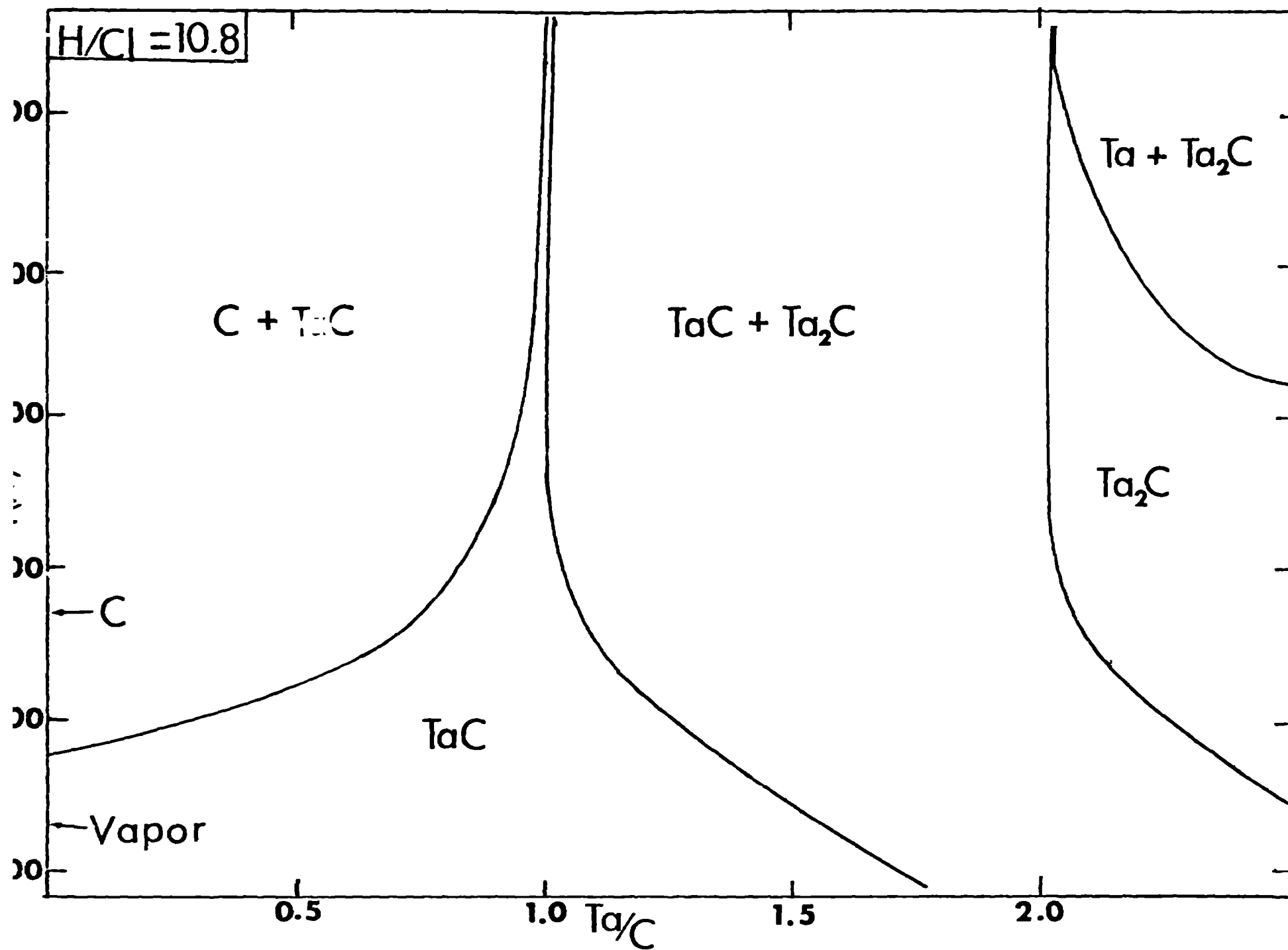


FIGURE 7



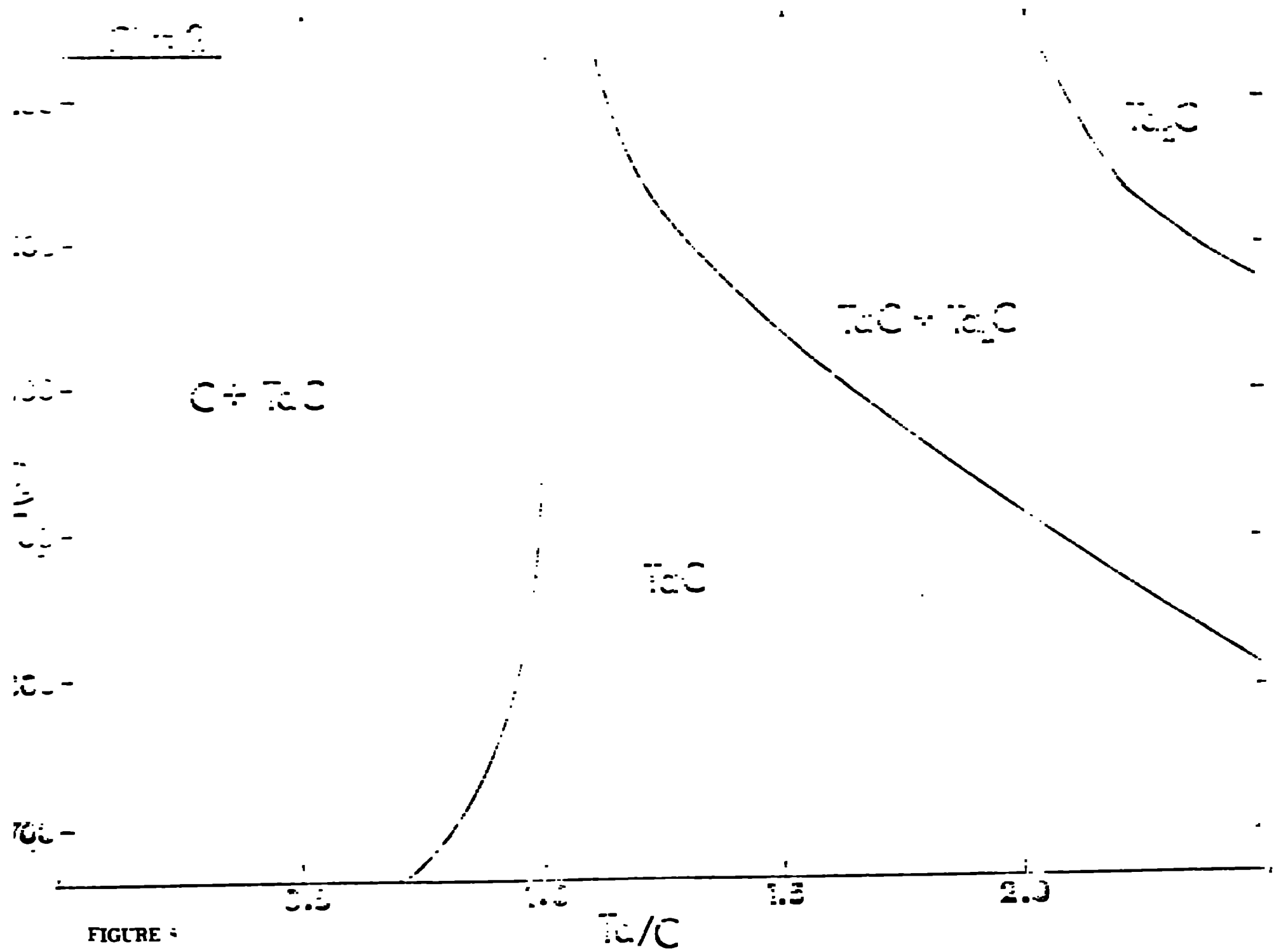


FIGURE 3

FIGURE 9

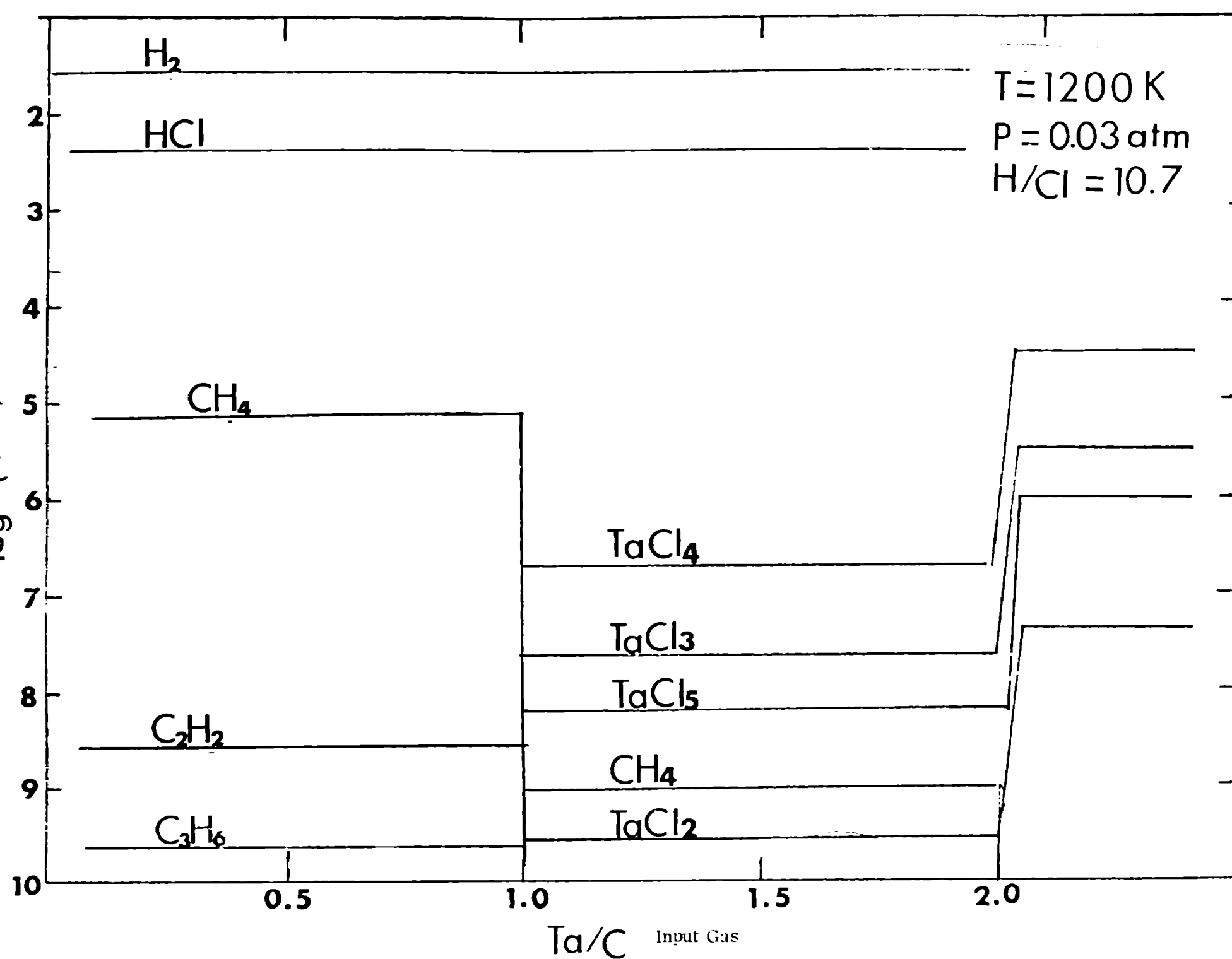


FIGURE 10

